32nd Annual International Conference of the IEEE EMBS
Buenos Aires, Argentina, August 31 - September 4, 2010

Acquisition of Action Potentials with Ultra-Low Sampling Rates

Lakshminarayan Srinivasan, Lav R. Varshney, and Julius Kusuma

Abstract— **We introduce finite rate of innovation (FRI) based spike acquisition, a new approach to the sampling of action potentials. Drawing from emerging theory on sampling FRI signals, our process aims to acquire the precise shape and timing of spikes from electrodes with single or multiunit spiking activity using sampling rates of 1000 Hz or less. The key insight is that action potentials are essentially stereotyped pulses that are generated by neurons at a rate limited by an absolute refractory period. We use this insight to push sampling below the Nyquist rate. Our process is a parametric method distinct from compressed sensing (CS). In its full implementation, this process could improve spike-based devices for neuroscience and medicine by reducing energy consumption, computational complexity, and hardware demands.**

I. Introduction

Action potentials, or spikes, are millisecond-width pulses of millivolt-scale electrochemical potential that propagate along neuronal cell membranes to facilitate rapid neuron-neuron communication over distances of millimeters to meters. Spikes are commonly emitted by individual neurons at rates between 0 and 100 Hz. Fully-implanted devices that access spikes are emerging to create new scientific and therapeutic opportunities.

Energy consumption represents a fundamental challenge to the success of spike-based devices. For each channel of spiking neural activity recorded, existing laboratory systems use sampling rates in excess of 16 kHz to adequately capture the shape and timing of spikes. Emerging applications require tens to hundreds of these channels. In contrast, cardiac arrhythmias can be detected with single-channel data and 500 Hz sampling rates. Compared to this historical precedent, present-day spike-based acquisition generates an energy burden that is orders of magnitude larger.

As an alternative to spike-based devices, many research groups have explored the use of local field potentials and other variants of electroencephalography (EEG). These recording modalities accommodate sampling rates below 1 kHz but offer a lower resolution view of brain activity. In comparison, a process that could achieve spike acquisition with sub-kilohertz sampling rates would produce a comparable reduction in power consumption while maintaining high spatial and temporal resolution. Unfortunately, spike acquisition based on Nyquist sampling is hard-limited by the action potential bandwidth (several kHz) rather than the spiking rate.

Manuscript received March 31, 2010. L. Srinivasan is a resident of San Diego, CA (e-mail: ls2@alum.mit.edu), L. R. Varshney is a resident of Cambridge, MA (e-mail: varshney@alum.mit.edu), and J. Kusuma is a resident of Somerville, MA (email: kusuma@alum.mit.edu).

Various algorithms have been explored to reduce data transmission rates compared to raw waveform transmission in wireless spike acquisition, but these methods do not reduce sampling rates [1]–[3]. Initially, spikes are band-pass-filtered and sampled at the usual Nyquist rate, typically more than 10 kHz. Subsequently, a compression algorithm condenses the digitized waveform prior to wireless transmission. Under this paradigm, the implanted device must still supply energy to perform sampling, buffering, and data compression at high rates. In contrast, our process aims to reduce energy requirements for both telemetry and *in situ* data acquisition and processing.

Recent work [4], [5] has begun to focus on directly reducing sampling rates in spike acquisition using the theory of compressed sensing (CS). CS was originally cast as a general, non-parametric sampling technique for sparse signals [6], [7]. Specifically, CS describes a method to sample and recover a length-N sequence z with $M = O(K \log(N/K))$ samples where z has $K < N$ non-zero entries in some basis. CS is a mathematically distinct framework from the approach that we illustrate here. The application of CS to spike acquisition is preliminary and ongoing. In marked contrast to CS, our new process for spike sampling draws on finite rate of innovation (FRI) theory, a fundamentally model-based approach that allows us to exploit biophysical constraints on action potential shape and timing.

In this paper, we formulate spike acquisition as the sampling of an FRI signal. The *rate of innovation* is the number of parameters needed on average to describe a signal per unit time. For example, the rate of innovation K in a sequence of pulses is given by the average number of pulses per unit time multiplied by the number of parameters that characterize each pulse. In prior work [8], [9], a class of parametric methods were developed to exploit the rate of innovation in a canonical set of FRI signals to achieve sampling rates of $M = O(K)$. This theory allows for temporal resolution that far exceeds the sampling rate but degrades with signal-to-noise ratio (SNR).

Here, we describe spiking data as an FRI signal, composed of a sequence of parameterized, variably shaped pulses embedded in background noise. In theory, innovation rates are bounded by the biophysically-confined refractory period and variations in action potential shape. Even for multi-unit activity, the average innovation rate can be significantly less than the absolute refractory period would suggest because neurons fire intermittently. As we estimate below, the requisite sampling rate with FRI-based spike acquisition can easily be as low as 400 Hz in a multi-unit electrode. This is significantly lower than the 5–8 kHz bandwidth of any

individual spike. Conventional techniques must sample at twice the spike bandwidth to preserve the spike train.

II. Spike Acquisition Process

A. Spiking Data as an FRI Process

Consider the case of one recording channel that receives action potentials from multiple neurons over a segment of time $[0, T)$. As a general approximation, the waveform on this channel is a signal composed of shifted and scaled pulses:

$$x(t) = \sum_{k=0}^{K-1} \sum_{l=0}^{L-1} g_{k,l}\left(t - t_{k,l}\right) + \varepsilon(t). \tag{1}$$

Here, k indexes the various time delays, l indexes the pulse shape as it varies across neurons, and $\varepsilon(t)$ represents noise. The full problem formulation seeks to recover the spike shapes $g_{k,l}$ and arrival times $t_{k,l}$ with a sampling scheme that achieves uniform-rate sub-Nyquist sampling.

As an initial step, we further simplify the spiking waveform into a summation of impulses with varying amplitudes and delays where noise is not modeled:

$$x(t) = \sum_{k=0}^{K-1} c_k \delta\left(t - t_k\right),\ c_k \in \mathbb{R},\ t_k \in [0, T). \tag{2}$$

For this discussion, we assume there are exactly K impulses in the T second interval. In practice, FRI-based spike acquisition still works if K is chosen to be larger than the actual number of spikes. The best choice of T will depend on background noise, device refresh rate, and other factors. Subsequent work will discuss optimal selection of K and T. With the spiking data described as an FRI signal, we now apply FRI sampling theory to produce a spike acquisition procedure.

B. FRI-Based Spike Sampling

In FRI-based spike acquisition, the signal is first passed through a bank of filters or "sampling kernels." Second, each of the filter outputs is sampled once at time T; these sample values are related to the signal parameters through a powersum series governed by the choice of filters. Third, the powersum series is solved to produce the signal parameters.

For the FRI signal form in (2), this process is particularly conducive to hardware implementation with passive components, because the sampling kernels can simply be successive integrals of the original signal $x(t)$ [10]:

$$\begin{aligned} x_0(t) &= \int_0^t x(\tau) d\tau, \\ x_{l+1}(t) &= \int_0^t x_l(\tau) d\tau, \end{aligned} \tag{3}$$

with samples

$$y_l = x_l(T) = \frac{1}{l!} \sum_{k=0}^{K-1} c_k (T - t_k)^l,\ l = 0, 1, \ldots, L-1. \tag{4}$$

C. Reconstructing Spikes from FRI-Based Spike Samples

The L integrated samples $\{y_l\}_{l=0}^{L-1}$ from (4) are sufficient to determine the time shifts $\{t_k\}_{k=0}^{K-1}$ and the amplitudes $\{c_k\}_{k=0}^{K-1}$ uniquely. This is because the samples define a powersum series $s_l = l! \cdot y_l$:

$$s_l = \sum_{k=0}^{K-1} c_k (T - t_k)^l,\ l = 0, 1, \ldots, L-1. \tag{5}$$

Recall that a powersum series is simply a series of the form:

$$r_l = \sum_{k=0}^{K-1} c_k (u_k)^l,\ l = 0, 1, \ldots, L-1, \tag{6}$$

where the c_k are called amplitudes and the u_k are called coefficients or poles. The correspondence between (5) and (6) is readily apparent. Prony first showed that amplitudes and coefficients $\{c_k, u_k\}_{k=0}^{K-1}$ of general powersums can be recovered exactly with $2K + 1$ observations [11]. His recovery process is called the annihilating filter method in the signal processing literature. For our illustration, we adapt elements of the annihilating filter implementation described in [8]. An annihilating filter is a finite impulse-response filter with $K+1$ coefficients $a_0, \ldots, a_K$. The recovery process is:

1) Solve for the annihilating filter coefficients $a_0, \ldots, a_K$ using the $2K+1$ FRI samples $s_0, \ldots, s_{2K}$ by forming

$$S = \begin{bmatrix} s_K & \cdots & s_1 & s_0 \\ s_{K+1} & \cdots & \cdots & s_1 \\ \vdots & \ddots & \ddots & \vdots \\ s_{2K} & \cdots & s_{K+1} & s_K \end{bmatrix},$$

and performing the singular value decomposition $S = U\Sigma V^*$. Then

$$\begin{bmatrix} a_0 \\ a_1 \\ \vdots \\ a_K \end{bmatrix} = V \begin{bmatrix} 0 \\ \vdots \\ 0 \\ 1 \end{bmatrix},$$

i.e. the last column of V corresponds to the annihilating filter coefficients.

2) Solve for the roots $\{u_k\}$ of the annihilating filter. The preliminary spike times are given by $t_k = T - u_k$.

3) Determine the spike amplitudes c_k. Proceed by solving the linear system in (5) with the $\{u_k\}$ computed in step 2:

$$\begin{bmatrix} 1 & 1 & \cdots & 1 \\ u_0 & u_1 & \cdots & u_{K-1} \\ \vdots & \vdots & \ddots & \vdots \\ u_0^{K-1} & u_1^{K-1} & \cdots & u_{K-1}^{K-1} \end{bmatrix} \begin{bmatrix} c_0 \\ c_1 \\ \vdots \\ c_{K-1} \end{bmatrix} = \begin{bmatrix} s_0 \\ s_1 \\ \vdots \\ s_{K-1} \end{bmatrix}.$$

In our illustration, we solve for c_k in the above equation using the pseudoinverse of the first matrix with u values: $c = U^\dagger s$.

4) Eliminate spurious spike times by expurgating t_k corresponding to c_k with complex values or amplitudes below a desired spike detection threshold.

Note that some implementations fix the a_0 filter coefficient to be 1 without loss of generality, so that only $L = 2K$ samples are required (rather than $L = 2K + 1$ above) [10].

D. Extension to Full Action Potential Recovery

The signal sampling and recovery process we have outlined can be extended to recover the full action potential shape. One way to extend this process is to model each action potential with a small number of Fourier series coefficients [9]. This capability will be useful to support more powerful spike sorting, and potentially to perform other unforeseen analyses. Due to space constraints, we will illustrate this process in future work.

E. Extension to Pulse Oximetry

Previous work has adapted FRI-based sampling techniques to electrocardiography (ECG) [12] and electroencephalography (EEG) [13]. In this section, we briefly describe FRI-based pulse oximetry (PO). PO is a non-invasive measure of blood oxygenation used widely in hospitals. As with spikes, PO waveforms are biophysically constrained. This is because red and infra-red absorbance at a given measurement point vary in a characteristic fashion with the hemodynamic flow as it depends on cardiovascular and pulmonary function. As a result, the basic PO waveform can be described as a sum of shifted pulses, which is amenable to FRI theory. One manifestation of this process is described in Section II-D. As alternate manifestations, more specific waveform models could be incorporated to describe the PO waveform. Wireless or ambulatory PO are target applications. Due to space limitations, we will illustrate FRI-based pulse oximetry in future work.

III. Demonstration

As a first demonstration of FRI-based spike acquisition, we examined its effect on the simulated performance of an upper-extremity neural prosthetic device. In this simulation, a third-order random walk (position, velocity, acceleration) is used to generate a smooth but undirected trajectory of 2.5 seconds in duration. This represents the intended movement of an "arm" which can be a robotic limb, computer cursor, or other actuator (black line in Fig. 1C). Next, spike times are simulated from 64 neurons using a point process stochastic model of primary motor cortical neurons [14], [15]:

$$\lambda(t|v_x, v_y) = \exp\left(\beta_0 + \beta_1\sqrt{v_x^2 + v_y^2}\cos(\theta - \theta_p)\right).$$

The user's brain modulates the firing rate (λ) of each neuron based on the intended arm velocity (v_x, v_y) in meters, with $\beta_0 = 2.28$ (unitless), $\beta_1 = 8.28$ s/m, and random uniform phase θ_p. This corresponds to background firing rates of 10 spikes/s, and firing rates of 50 spikes/s at a speed of 0.2 m/s in the preferred direction. For simplicity, we idealize these action potentials as instantaneous delta functions with area of 1 normalized unit (unitless). We then generate FRI samples based on these spike times for $L = 3$ and a sampling rate of 1 kHz. These samples are corrupted by additive Gaussian noise at varying SNR as depicted in Fig. 1A. The noise

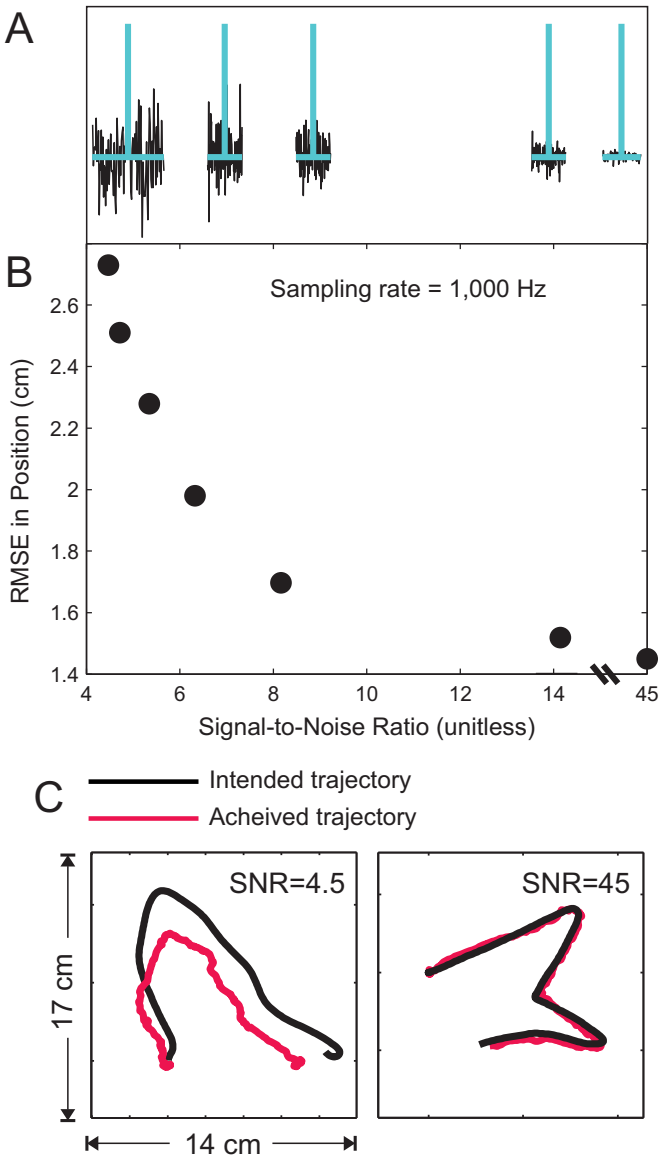

Fig. 1. A first demonstration of FRI-based spike sampling in the presence of noise. (A) Examples of additive Gaussian noise (black) in the $x_0(t)$ FRI sample compared with the unit integrated area from a single spike (blue) at various SNR from the electrode channel. (B) Root mean squared error (RMSE) in position decoding at various SNR (linear scale). (C) Typical trajectories of a simulated prosthetic limb at two different SNR, each lasting 2.5 s in duration.

model assumes a serial configuration of integrators, so that the noise terms $(w_0(t), w_1(t), w_2(t))$ added to FRI samples $(x_0(t), x_1(t), x_2(t))$ at each sampling time are zero-mean jointly Gaussian random variables with cross-correlation:

$$E\left[w_l(t)w_k(t)\right] = \frac{N_0}{2}\frac{1}{k+l+1}T^{k+l+1}, \qquad (7)$$

where $N_0/2$ is the noise spectral density, T is the sampling period, and l and k index the corresponding noise terms [10].

Spike times are recovered from the noise-corrupted FRI samples using the 4-step process outlined in Section II-C. Finally, a recursive Bayesian approximate point process filter estimates the intended trajectory [16] (red line in

Fig. 1C). This filter uses exact neuronal parameter values and a second-order random walk for the trajectory model.

The simulated result illustrates the feasibility of our FRI spike acquisition process, predicts that performance will degrade with spike-to-background SNR, and provides specific context by illustrating its relevance to one particular spike-based device. Unfortunately, space limitations restrict us from providing additional detail regarding the simulation. We expect these basic conclusions to hold across a variety of simulated conditions that the reader may choose to investigate. Previous articles provide a more complete discussion on simulating primary motor cortical neurons [15], [17], implementing a basic point process recursive Bayesian estimation filter [16], and connecting these elements for in silico validation of neural prosthetic algorithms [17], [18].

IV. Conclusions and Future Work

In this paper, we introduced a new approach to spike acquisition aimed at reducing power consumption in spike-based devices without sacrificing performance. The critical step in this process was to approximate single- or multi-unit spiking data as finite rate of innovation signals. Subsequently, we outlined a general approach for spike acquisition, including a specific manifestation where spiking data is modeled as a sequence of shifted and scaled delta functions. This example was further illustrated in the operation of a spike-based neural prosthetic device for limb control based on simulated neural activity from primary motor cortex.

With further development, FRI-based spike acquisition may be able to achieve the goal of sub-kilohertz sampling. A rough calculation using hippocampal tetrode data [19] illustrates the feasibility of this goal. A single channel from the tetrode records spikes from 2 to 3 neurons at once, but accumulates fewer than 100 spikes per second in total. Moreover, the simple peak-to-peak amplitude feature of the spike alone can be used to discriminate between multiple neurons through spike sorting [19]. Accordingly, the rate of innovation is approximately 200 parameters per second, since there are approximately 100 spike times per second and 100 peak-to-peak amplitude values per second. By extending FRI theory to this setting, a best-case scenario might achieve sampling rates as low as 400 Hz without degrading the capability for spike sorting.

Subsequent design and validation studies are needed to further refine and test FRI-based spike acquisition. To this end, simulated and experimentally-recorded neural data will provide complementary information. Parallel developments in CS-based spike acquisition will serve as important points of comparison. Finally, the precise impact of FRI methods on energy consumption, computational complexity, and circuit complexity requires thorough investigation.

Sampling at reduced rates should be a key goal in spike-based device engineering because it decreases resource demands in all parts of the system: acquisition, processing, and telemetry. Our calculations suggest that FRI-based spike acquisition is positioned to address this important design challenge.

References

[1] C. H. Chung, L.-G. Chen, Y.-C. Kao, and F.-S. Jaw, "Optimal transform of multichannel evoked neural signals using a video compression algorithm," in *Proc. 3rd Int. Conf. Bioinformatics Biomed. Eng. (ICBBE 2009)*, June 2009.

[2] S. Craciun, D. Cheney, K. Gugel, J. C. Sanchez, and J. C. Principe, "Compression of neural signals using discriminative coding for wireless applications," in *Proc. 4th Int. IEEE/EMBS Conf. Neural Eng. (NER'09)*, Apr.-May 2009, pp. 629–632.

[3] K. G. Oweiss, "A systems approach for data compression and latency reduction in cortically controlled brain machine interfaces," *IEEE Trans. Biomed. Eng.*, vol. 53, pp. 1364–1377, July 2006.

[4] C. Hegde, M. F. Duarte, and V. Cevher, "Compressive sensing recovery of spike trains using a structured sparsity model," in *Proc. Signal Process. Adaptive Sparse Structured Representations (SPARS'09)*, Apr. 2009.

[5] C. Hegde and R. G. Baraniuk, "Compressive sensing of streams of pulses," in *Proc. 47th Annu. Allerton Conf. Commun. Control Comput.*, Sept.-Oct. 2009, pp. 44–51.

[6] E. J. Candes and T. Tao, "Near-optimal signal recovery from random projections: Universal encoding strategies?" *IEEE Trans. Inf. Theory*, vol. 52, pp. 5406–5425, Dec. 2006.

[7] D. L. Donoho, "Compressed sensing," *IEEE Trans. Inf. Theory*, vol. 52, pp. 1289–1306, Apr. 2006.

[8] M. Vetterli, P. Marziliano, and T. Blu, "Sampling signals with finite rate of innovation," *IEEE Trans. Signal Process.*, vol. 50, pp. 1417–1428, June 2002.

[9] J. Kusuma, I. Maravić, and M. Vetterli, "Sampling with finite rate of innovation: Channel and timing estimation for UWB and GPS," in *Proc. IEEE Int. Conf. Commun. (ICC 2003)*, May 2003, pp. 3540–3544.

[10] J. Kusuma, "Economical sampling of parametric signals," Ph.D. thesis, Massachusetts Institute of Technology, Cambridge, MA, Sept. 2006.

[11] R. Prony, "Essai expérimental et analytique: Sur les lois de la dilatabilité des fluides élastiques et sur celles de la force expansive de la vapeur de l'eau et de la vapeur de l'alkool, à différentes températures," *J. École Polytechnique Floréal Plairial*, vol. 1, pp. 24–76, 1795.

[12] Y. Hao, P. Marziliano, M. Vetterli, and T. Blu, "Compression of ECG as a signal with finite rate of innovation," in *Proc. 27th Annu. Int. Conf. Eng. Medicine Biology Soc. (IEEE-EMBS 2005)*, Jan. 2006, pp. 7564–7567.

[13] K.-K. Poh and P. Marziliano, "Compression of neonatal EEG seizure signals with finite rate of innovation," in *Proc. IEEE Int. Conf. Acoust., Speech, Signal Process. (ICASSP 2008)*, Mar.-Apr. 2008, pp. 433–436.

[14] D. W. Moran and A. B. Schwartz, "Motor cortical representation of speed and direction during reaching," *J. Neurophysiol.*, vol. 82, pp. 2676–2692, Nov. 1999.

[15] W. Truccolo, U. T. Eden, M. R. Fellows, J. P. Donoghue, and E. N. Brown, "A point process framework for relating neural spiking activity to spiking history, neural ensemble, and extrinsic covariate effects," *J. Neurophysiol.*, vol. 93, pp. 1074–1089, Feb. 2005.

[16] U. T. Eden, L. M. Frank, R. Barbieri, V. Solo, and E. N. Brown, "Dynamic analysis of neural encoding by point process adaptive filtering," *Neural Comput.*, vol. 16, pp. 971–998, May 2004.

[17] L. Srinivasan, U. T. Eden, A. S. Willsky, and E. N. Brown, "A state-space analysis for reconstruction of goal-directed movements using neural signals," *Neural Comput.*, vol. 18, pp. 2465–2494, Oct. 2006.

[18] L. Srinivasan, U. T. Eden, S. K. Mitter, and E. N. Brown, "General-purpose filter design for neural prosthetic devices," *J. Neurophysiol.*, vol. 98, pp. 2456–2475, Oct. 2007.

[19] D. Ji and M. A. Wilson, "Firing rate dynamics in the hippocampus induced by trajectory learning," *J. Neurosci.*, vol. 28, pp. 4679–4689, Apr. 2008.